The Journal of Chemical Physics

High-pressure behavior of bromine confined in the one-dimensional channels of zeolite $AlPO_4$-5 single crystals

Cite as: J. Chem. Phys. **145**, 124319 (2016); https://doi.org/10.1063/1.4963725
Submitted: 02 June 2016 . Accepted: 15 September 2016 . Published Online: 30 September 2016

Zhaodong Liu, Zhen Yao, Mingguang Yao, Jiayin Lv, Shuanglong Chen, Quanjun Li, Hang Lv, Tianyi Wang, Shuangchen Lu, Ran Liu, Bo Liu, Jing Liu, Zhiqiang Chen, Bo Zou, Tian Cui, and Bingbing Liu

High-pressure behavior of bromine confined in the one-dimensional channels of zeolite $AlPO_4$-5 single crystals

Zhaodong Liu,[1,a),b)] Zhen Yao,[1,2,b)] Mingguang Yao,[1] Jiayin Lv,[1] Shuanglong Chen,[1] Quanjun Li,[1] Hang Lv,[1] Tianyi Wang,[1] Shuangchen Lu,[1] Ran Liu,[1] Bo Liu,[1] Jing Liu,[3] Zhiqiang Chen,[4] Bo Zou,[1] Tian Cui,[1] and Bingbing Liu[1,c)]

[1]*State Key Laboratory of Superhard Materials, Jilin University, Changchun 130012, China*
[2]*College of Science, Liaoning University of Technology, Jinzhou, Liaoning 121001, China*
[3]*Beijing Synchrotron Radiation Facility, Institute of High Energy Physics, Chinese Academy of Sciences, Beijing 100049, China*
[4]*Geoscience Department, Stony Brook University, Stony Brook, New York 11794, USA*

(Received 2 June 2016; accepted 15 September 2016; published online 30 September 2016)

We present a joint experimental and theoretical study on the high-pressure behavior of bromine confined in the one-dimensional (1D) nanochannels of zeolite $AlPO_4$-5 (AFI) single crystals. Raman scattering experiments indicate that loading bromine into AFI single crystals can lead to the formation of bromine molecular chains inside the nanochannels of the crystals. High-pressure Raman and X-ray diffraction studies demonstrate that high pressure can increase the length of the confined bromine molecular chains and modify the inter- and intramolecular interactions of the molecules. The confined bromine shows a considerably different high-pressure behavior to that of bulk bromine. The pressure-elongated bromine molecular chains can be preserved when the pressure is reduced to ambient pressure. Theoretical simulations explain the experimental results obtained from the Raman spectroscopy and X-ray diffraction studies. Furthermore, we find that the intermolecular distance between confined bromine molecules gradually becomes comparable to the intramolecular bond length in bromine molecules upon compression. This may result in the dissociation of the bromine molecules and the formation of 1D bromine atomic chains at pressures above 24 GPa. Our study suggests that the unique nanoconfinement has a considerable effect on the high-pressure behavior of bromine, and the confined bromine species concomitantly enhance the structural stability of the host AFI single crystals. *Published by AIP Publishing.* [http://dx.doi.org/10.1063/1.4963725]

I. INTRODUCTION

Simple molecular solid systems represent an important topic for high-pressure physics and chemical science.[1–3] The application of pressure on these systems forces the molecules to approach each other until the intermolecular distances become comparable to the distances between atoms in a molecule. This causes the molecules to lose their identity, and results in molecular dissociation and metallization.[1–9] Bromine, a typical diatomic molecule, is a key constituent of simple molecular solids. It is believed to undergo earlier pressure-induced metallization and dissociation transitions than solid molecular hydrogen (H_2).[7–9] Thus, the high-pressure study of bromine (Br_2) molecules is of great importance for understanding the molecular dissociation and metallization of diatomic molecules, and could have a considerable impact on the investigation of these phenomena in solid H_2.

Recent high-pressure studies on diatomic molecules confined in the nanospace provide new insights for the further exploration of the physical properties of diatomic molecular systems.[10–13] Trapping diatomic molecules in one-dimensional (1D) nanochannels is an effective way to fabricate long and stable atomic or molecular arrays.[10–16] Such arrays exhibit considerably different physical properties, such as coordination[10,11] and bond lengths,[12,13] to their bulk counterparts and have great potential for application in nanoscale devices.[10–17] Br_2 molecules have been intercalated into nanochannel-containing materials such as carbon nanotubes[18,19] and silicon clathrates.[20] Polybromide chains have been shown to exist within carbon nanotubes,[18] and inhomogeneous loading of these nanotubes with bromine can even reduce the high-pressure stability of the host.[19] This is in contrast to the increase of structural stability of other nanospace materials doped with diatomic molecules, such as silicon clathrates[20] and zeolite single crystals[12,13,16] doped with I_2, or zeolite single crystals doped with N_2.[21] A recent study suggested that Br_2 molecules (van der Waals diameter = 0.40 nm) can be loaded into zeolite $AlPO_4$-5 (AFI) single crystals to form bromine molecular chains inside the 1D nanochannels of the crystal (inner diameter = 0.73 nm).[22] The uniform 1D hexagonal-packed channels of the AFI single crystal provide an ideal basis from which to explore the pressure behavior of confined bromine at a molecular level and to study the effects of the confined bromine on the structural stability of the AFI host.

Under high pressure, bulk Br_2 molecules are first transformed from a molecular phase (phase I) into phase I′ at 25 GPa, with a loss of molecular character caused

[a)]Present address: Bayerisches Geoinstitut, University of Bayreuth, 95440 Bayreuth, Germany.
[b)]Z. Liu and Z. Yao contributed equally to this work.
[c)]Electronic mail: liubb@jlu.edu.cn

by the change of the intramolecular bonds,[8,23–25] then to an incommensurate phase (phase V) at 84 GPa,[7–9,26] and an atomic phase (phase II) at 115 GPa.[8,9] Theoretically, the pressure evolution of bromine upon compression will be affected by its presence in the confined nanochannels of the AFI single crystals. However, the high-pressure behavior of bromine in nanoconfinement is still unclear. A high-pressure Raman and X-ray diffraction (XRD) study on bromine confined inside the 1D nanochannels of AFI single crystals can therefore provide us with a new understanding of the physical properties of bulk bromine and bromine-intercalated compounds.

Here, we use *in situ* Raman spectroscopy, synchrotron XRD, and theoretical simulations to study the high-pressure behavior of bromine species confined within the 1D nanochannels of AFI single crystals. We also report the effects of bromine loading on the structural stability of the host crystals.

II. EXPERIMENTAL AND THEORETICAL METHODS

The AFI single crystals were doped with bromine, which was loaded into the channels of the AFI structure, using physical vapor diffusion methods. The experimental details can be found elsewhere.[22] The doped samples had a yellow-gold color, in contrast to the colorless AFI single crystals (see supplementary material, Fig. S1). The bromine-doped AFI single crystals (Br@AFI) were then heated at 59 °C for 2 h to remove the Br_2 molecules adsorbed on the surface of the crystal. The Br@AFI samples can be preserved for at least 3 weeks in air at room temperature, as shown by our study of their Raman spectra (Fig. S2 of the supplementary material). We also measured the concentration of bromine loaded into the 1D nanochannels of the AFI single crystals using Raman spectroscopy (Fig. S3 of the supplementary material). AFI single crystals containing high concentrations of intercalated bromine were kept in a vacuum box before high-pressure experiments (Figs. S2 and S3 of the supplementary material).

The doped samples were characterized by Raman spectroscopy on an inVia Raman microscope (Renishaw, U.K.) using an argon ion laser (λ = 514 nm) as the excitation source and a wavelength-specific holograph notch filter with a cut-off of approximately 100 cm^{-1}. The laser power was set to 0.8 mW, and the laser analysis spot size was about 3 μm in diameter using a 50× objective. *In situ* high-pressure Raman scattering and XRD measurements were conducted in a diamond anvil cell with a culet size of 500 μm. A T301 stainless steel gasket was preindented to 60 μm, and then a center hole of 150 μm in diameter was drilled to make the sample chamber. The claviform doped samples were transferred into this sample chamber, and tiny ruby chips were placed around the sample for pressure calibration. Liquid argon was used as the pressure transmission medium to provide a quasi-hydrostatic pressure environment. The angle-dispersive XRD measurements were performed at the 4W2 beamline of the Beijing Synchrotron Radiation Facility (λ = 0.4066 Å) and the X17C beamline of Brookhaven National Laboratory (λ = 0.406 17 Å). XRD patterns were integrated to give 1D powder diffraction patterns using the FIT2D program.[27]

For the theoretical simulation, a unit cell that contained three equally spaced Br_2 molecules lying along the center of a channel in the AFI lattice was constructed (Fig. 1). The initial lattice parameters *a*, *b*, *c*, and unit cell volume *V* of this unit cell were 14.0915 Å, 14.0915 Å, 17.4352 Å, and 2998.27 $Å^3$, respectively. For the purpose of constructing the

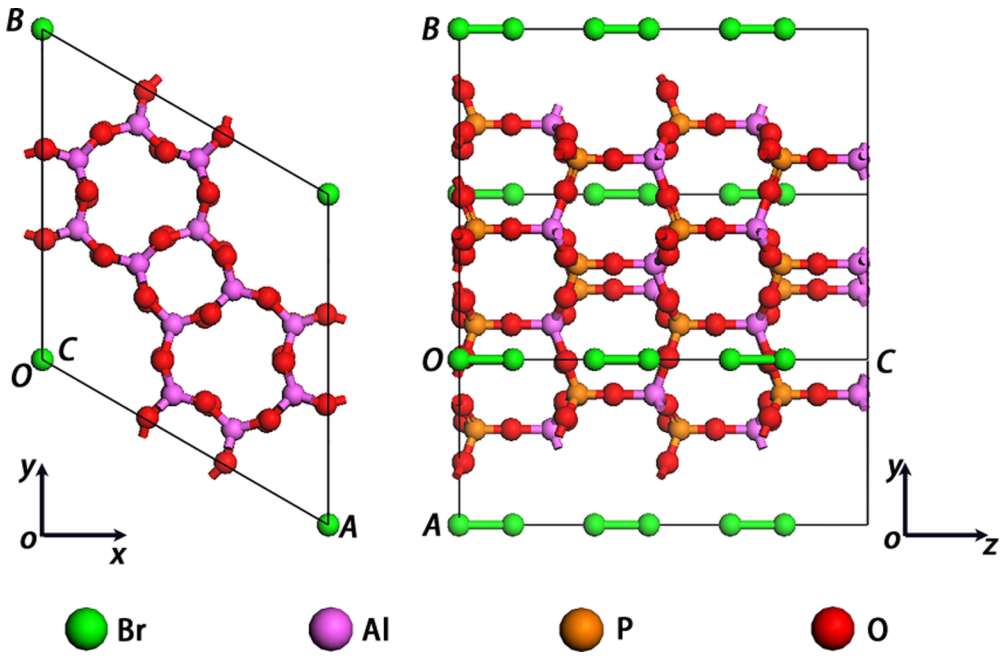

FIG. 1. The constructed periodic unit with three equally spaced bromide molecules lying on the channel center used in the simulation. The left and right images are the projections in the (x, y) and (y, z) planes, respectively.

1D periodic structure of the Br_2 molecules, the theoretical value of c was set to two times that of the experimental value.[22] The intramolecular bond length and separation between two adjacent Br_2 molecules were 2.305 Å and 3.490 Å, respectively. Calculations were performed within the generalized gradient approximation of density functional theory. We employed the Vienna *ab initio* simulation package program[28] and used a norm-conserving pseudo-potential with an energy cutoff of 520 eV. The Brillouin zone integration was performed using the Monkhorst-Pack scheme with $1 \times 1 \times 1$ k-points.[29] Following our experimental analysis, we performed the structural optimization up to 32 GPa.

III. RESULTS AND DISCUSSION

Raman spectra of Br@AFI and AFI single crystals under ambient conditions are shown in Fig. 2. Because the original AFI samples were calcined at 580 °C in an O_2 atmosphere for 24 h to remove the tripropylamine [$(CH_3CH_2CH_3)N$] templates,[22,28] there are no observable Raman signals for the pure AFI single crystals in the studied frequency region.[30] Therefore, the new Raman peaks at 208, 265, and 314 cm^{-1} in the low-frequency region and the harmonic series ($2w_0$, $3w_0$) of the w_0 = 314 cm^{-1} peak appearing in the high-frequency region of the spectrum of the Br@AFI single crystals must originate from the bromine species. The positions and numbers of these Raman modes are almost the same as those obtained in our previous Raman study using a He–Ne laser (λ = 633 nm) as the excitation source.[22] It has been suggested that the most intense Raman vibration mode at 265 cm^{-1} could be assigned to the vibrational mode of $(Br_2)_n$ ($n \geq 2$) chains.[22] The large redshift of this Raman frequency compared with that observed in the spectrum of bulk bromine is caused by the stable bromine chains formed inside the AFI channels.[22] The Raman mode at 314 cm^{-1} originates from the intramolecular vibration of the individual Br_2 molecules, and shows a redshift compared with the corresponding mode of vapor-like Br_2 (320 cm^{-1}) owing to the confinement effect of the AFI nanochannels.[22] This is similar to the behavior observed for I_2 molecules in AFI nanochannels.[12,16] The weak Raman shoulder at 208 cm^{-1} can be attributed to that of the asymmetric

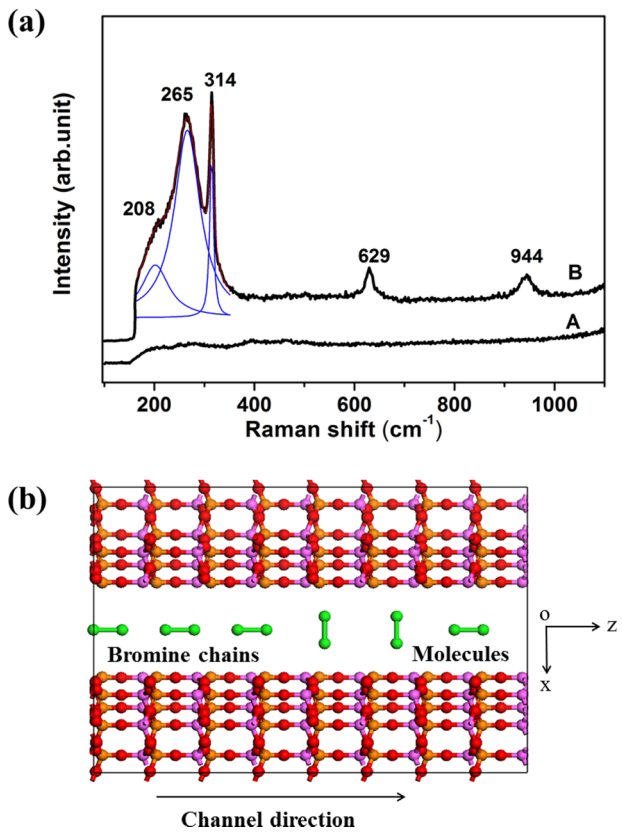

FIG. 2. (a) Raman spectra of one pristine AFI (a) and Br@AFI single crystals (b) at ambient conditions. Black lines correspond to the experimental data, blue lines are the different peaks used in the Lorentz fitting, and red lines are the total fitting results. (b) The schematic image of bromine chains and individual bromine molecules inside the 1D nanochannels of AFI single crystals. The green, red, yellow, and pink circles represent the atoms of bromine, oxygen, phosphorus, and aluminum, respectively.

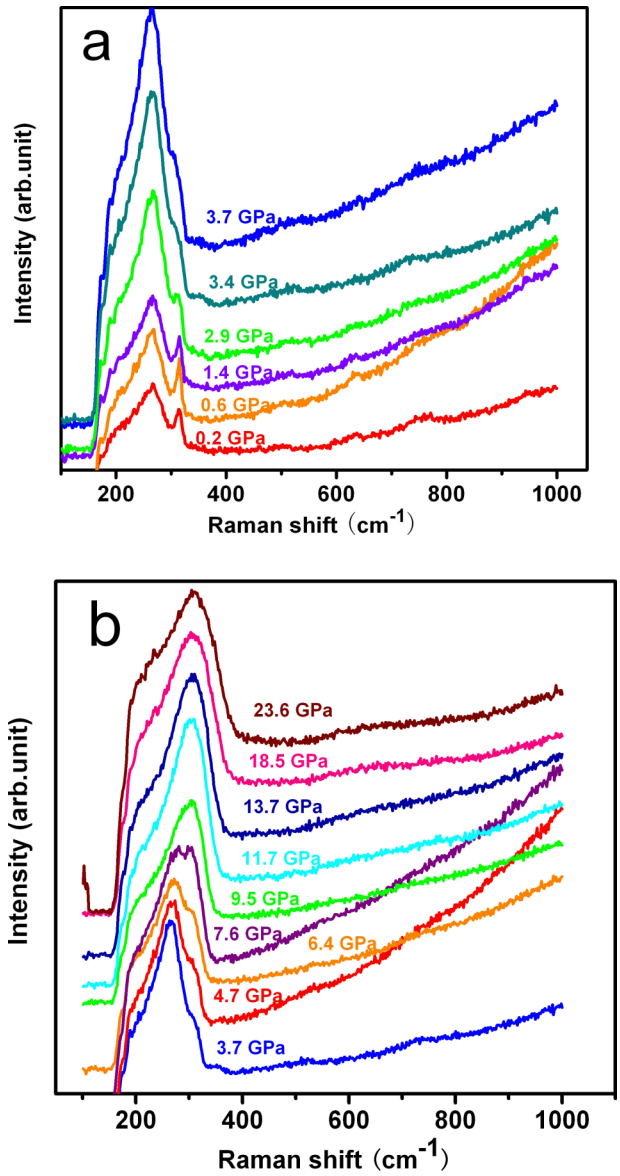

FIG. 3. High-pressure Raman spectra of a Br@AFI single crystal at various pressures. The Raman spectra at high pressures are stacked by shifting in vertical.

Br_3^- chains, which formed due to the charge transfer between bromine species and crystal defects or residual carbonaceous clusters inside the channels.[12,16,22] The assignment of these Raman modes has been confirmed by using polarized Raman measurements with an Ar-ion laser (λ = 514 nm) (Fig. S4 of the supplementary material) in the present study and a He–Ne laser (λ = 633 nm).[22]

The high-pressure behavior of bromine species inside the 1D nanochannels of AFI single crystals was studied by Raman scattering measurements combined with a diamond anvil cell. Raman spectra of a Br@AFI single crystal under high pressure are fitted with Lorentzian functions as three Raman modes in the low-frequency region (Fig. S5 of the supplementary material). The pressure evolution of the Raman peaks of $(Br_2)_n$ chains and Br_2 molecules is shown in Fig. 3. With increasing pressure, the Raman frequency of the $(Br_2)_n$ chains shifts gradually to the higher frequency, whereas that of the individual Br_2 molecules shifts to the lower frequency (Figs. 3 and 4(a)). This change is concomitant with an increase in the Raman intensity ratio between $(Br_2)_n$ chains and Br_2 molecules (Figs. 3 and 4(b)). At 3.7 GPa, the intensity of the Raman mode of the $(Br_2)_n$ chains becomes much stronger than that of the Br_2 molecules, and the corresponding Raman intensity ratio reaches a maximum. This indicates that the $(Br_2)_n$ chains are lengthened or the population of chains is increased at this pressure, which is similar to the behavior of confined $(I_2)_n$ ($n \geq 2$) chains.[12,16] At pressures higher than 3.7 GPa, the intensity ratio decreases. At 9.5 GPa, the Raman peaks of the $(Br_2)_n$ chains and the Br_2 molecules merge into one

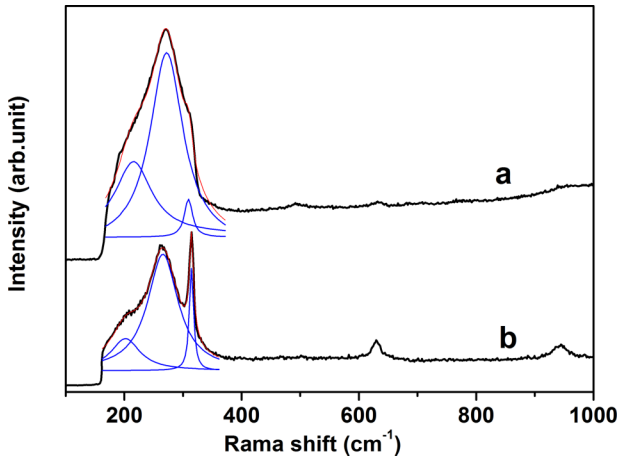

FIG. 5. Raman spectra of a Br@AFI single crystal upon decompression to ambient pressure (a) and before compression (b). Black lines correspond to the experimental data, blue lines are the different peaks used in the Lorentzian fitting, and red lines are the total fitting results.

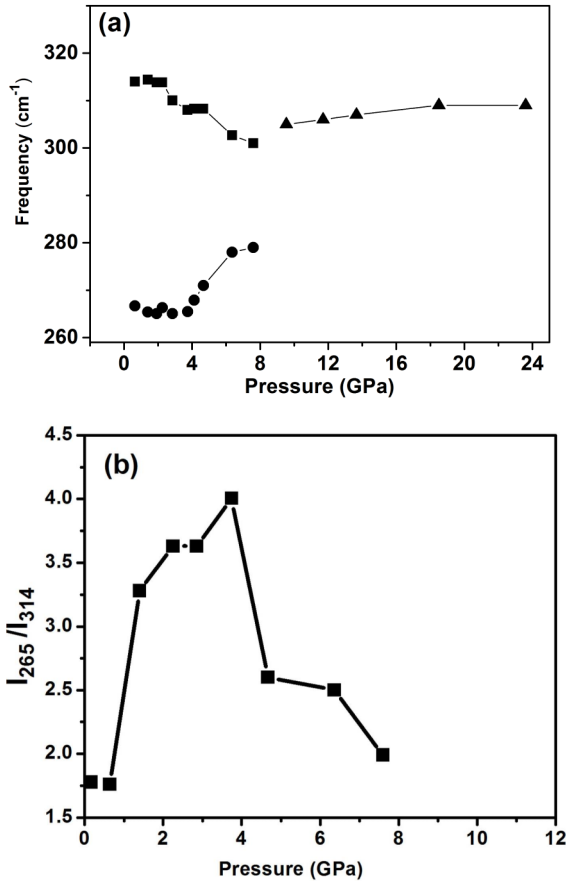

FIG. 4. (a) The pressure dependence of the Raman modes at 265, 314, and 305 cm^{-1}, which are represented by the circle, square, and triangle solid symbols, respectively. (b) The intensity ratio of Raman modes for $(Br_2)_n/Br_2$ as a function of pressure.

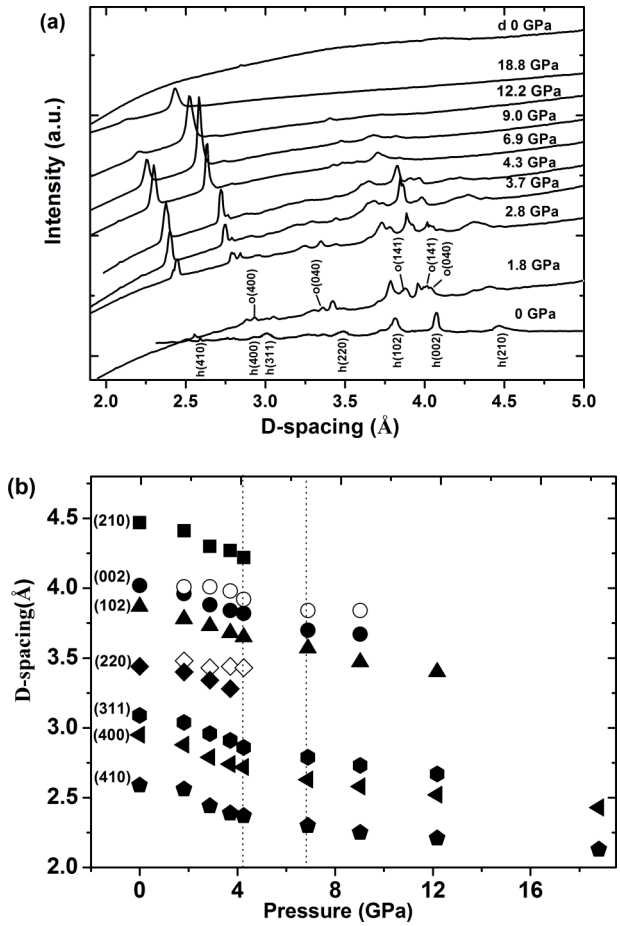

FIG. 6. (a) X-ray diffraction patterns of Br@AFI single crystals under high pressure. (b) Pressure dependence of d-spacing of Br@AFI single crystals.

broad Raman peak at 305 cm^{-1}, suggesting that the bromine species are in a different state inside the nanochannels. This Raman peak becomes gradually broader at pressures above 9.5 GPa and is retained up to 23.6 GPa. The present Raman spectroscopy results suggest that increased pressure induces a strong modification of the confined bromine species. We also note that the positions of these Raman peaks, as well as the evolution of their pressure behavior, clearly differ from those of bulk bromine,[8,31,32] as an additional evidence for the intercalation process.

After the sample was released from a pressure of 23.6 GPa, its Raman spectrum is slightly different with that observed before compression, and a relatively strong Raman mode at 270 cm^{-1} was observed (Fig. 5). This Raman mode shifts slightly to the higher frequency by about 5 cm^{-1} with respect to that observed before compression (265 cm^{-1}, Fig. 5). This shift may be caused by the weak interaction between the prolonged $(Br_2)_n$ chains and the deformed AFI channels. In the released Br@AFI sample, the Raman intensity of the $(Br_2)_n$ chains is considerably stronger than that of the Br_2 molecules. In addition, the Raman intensity of the $(Br_2)_n$ chains after decompression is much stronger than that observed before compression, whereas the Raman intensity of the Br_2 molecules is considerably lower. This suggests that the pressure-prolonged bromine chains formed in the deformed channels of AFI single crystals can be preserved at ambient pressure.

To investigate the effects of nanoconfinement on the bromine species and the effects of bromine intercalation on the framework stability of the AFI single crystals, we performed *in situ* XRD measurements on the Br@AFI samples. The XRD peaks of Br@AFI single crystals under ambient conditions (Fig. 6(a)) can be indexed as a hexagonal structure. New peaks are observed at 1.8 GPa and can be assigned to the diffractions of an orthorhombic structure.[31] This result suggests that the doped AFI single crystals transform into mixed phases of hexagonal and orthorhombic structures at 1.8 GPa, which is consistent with the behavior observed for pristine AFI single crystals.[33] At pressures above 9.0 GPa, most of the diffraction peaks disappear, and only the (410) and (400) diffraction peaks remain at 18.8 GPa. We can clearly see that the framework stability of the bromine-doped AFI single crystals is much higher than that of the empty AFI single crystals. This can be attributed to the support of the bromine species filling the pores, and agrees with our recent high-pressure studies of I_2@AFI[12] and N_2@AFI.[21]

The variation in the lattice parameters of the doped AFI single crystals at high pressures shows that the *a*-axis is less compressible than the *c*-axis below 4 GPa, but becomes more compressible than the *c*-axis at pressures above 4 GPa (Fig. S6 of the supplementary material). This result suggests that initial anisotropic compression along the channel direction (along the *c*-axis) will reduce the distance between neighboring molecules or between $(Br_2)_n$ chains and Br_2 molecules. This will in turn lead to the formation of longer $(Br_2)_n$ chains as well as an increased population of $(Br_2)_n$ chains, and can be further illustrated by theoretical calculations. As a result, a considerable increase in the Raman intensity ratio (chains/molecules) at 3.7 GPa is observed (Fig. 4), which is accompanied with a sudden change in the slope of the curves of AFI d-spacing vs. pressure (Fig. 6(b)) and AFI unit-cell volume vs. pressure at around 4 GPa (Fig. S7 of the supplementary material). Above 4 GPa, the *a*-axis becomes more compressible than the *c*-axis, which suggests that a

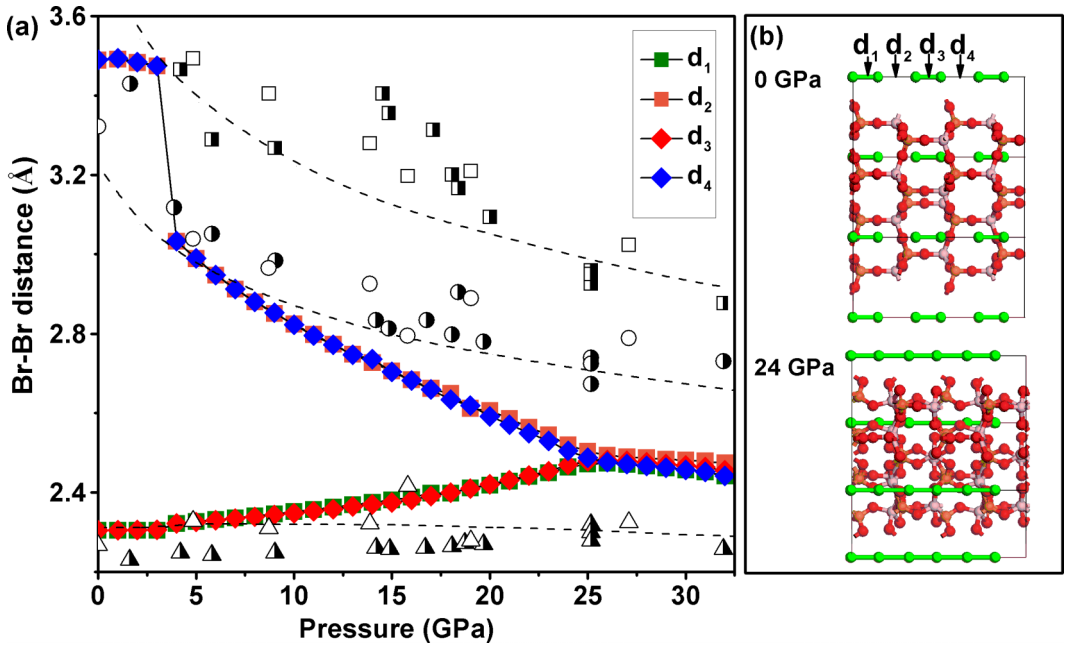

FIG. 7. (a) The confined bromine molecular distance evolution with pressures in the present calculation. Solid olivine and red symbols represent the bond length of the confined bromine molecules, and yellow and blue symbols represent the intermolecular distance between molecules. The open and half-filled symbols represent the experimental results of the bulk bromine molecules by using X-ray diffraction[26] and X-ray absorption spectroscopy experiments,[24] respectively. The dashed lines represent one previous theoretical result.[9] (b) Some representative schematic illustrations of bromine chains along the 1D channels of AFI framework at 0 and 24 GPa. The green, red, yellow, and pink circles represent the atoms of bromine, oxygen, phosphorus, and aluminum, respectively.

gradual ovalization of the AFI channels occurs. A similar phenomenon is also observed in AFI single crystals doped with iodine.[12] Another reduction in the AFI unit-cell volume occurs at around 9 GPa. This structural change should further enhance the interaction between the confined bromine species and the nanochannels, and thus affect the Raman frequency of the confined bromine species. These results can explain the discontinuity in the Raman frequency for the $(Br_2)_n$ chains and Br_2 molecules at 9.5 GPa, which is comparable to that observed for $(I_2)_n$ chains inside the nanochannels of AFI single crystals.[12] We therefore suggest that the Raman frequency of 305 cm^{-1} at 9.5 GPa may originate from the $(Br_2)_n$ chains inside the deformed AFI nanochannels. All of the Raman and XRD results in the present study suggest that nanoconfinement has an important effect on the high-pressure behavior of bromine species.

Theoretical simulations were then conducted to illustrate the effects of pressure on the bromine species inside the 1D nanochannels of the AFI single crystals. In Fig. 7, the pressure evolution of the intramolecular and intermolecular distances of the confined Br_2 molecules in the present study show a significant difference from those of bulk bromine molecules using the theoretical calculation,[9] X-ray diffraction,[26] and X-ray absorption spectroscopy experiments.[23,24] The intermolecular distance (d_2 and d_4) between adjacent Br_2 molecules inside the AFI channels decreases with increasing pressure and exhibits a sharp drop at about 4 GPa; this can be interpreted as a result of the collapse of the channel structure (Fig. 6 and Fig. S7 of the supplementary material). In contrast, the intramolecular bond lengths (d_1 and d_3) of the confined Br_2 molecules gradually increase with increasing pressure. This means that the Br_2 molecules rotate so that they lie along the 1D channel direction at increased pressures, and in doing so enhance the interaction between adjacent Br_2 molecules. This results in the prolongation of the molecular $(Br_2)_n$ chains and an increase in the population of chains inside the nanochannels of the AFI single crystals. Collapses occur in the unit-cell volume of the doped AFI single crystals at around 3.7 and 9 GPa in the present calculation (Fig. S7 of the supplementary material), and indicate that AFI may transform to a lower symmetry structure (hexagonal *P*6*cc*) or an orthorhombic structure (e.g., that of $AlPO_4$-11 with elliptical channels) at these pressures.[12,13] Thus, the present theoretical calculation, together with the XRD study, provides convincing support for the hypothesis that the increase in Raman intensity of the $(Br_2)_n$ chains at 3.7 GPa and the sharp increase of the Raman frequencies of the $(Br_2)_n$ chains at 9.5 GPa are due to the collapse of the AFI channels.

To interpret the mechanism of formation of the 1D bromine atomic chains, we also performed an electron localization function (ELF) calculation as a function of pressure. As shown in Fig. 8, the charge is mainly distributed on the isolated Br_2 molecules, and no charge is found between the adjacent molecules. Therefore, the pressure-induced transitions in the bromine species inside the AFI channels mainly result from topological transformations of the $(Br_2)_n$ chains and Br_2 molecules. When the pressure is increased to 19 GPa, a strong charge overlap is observed

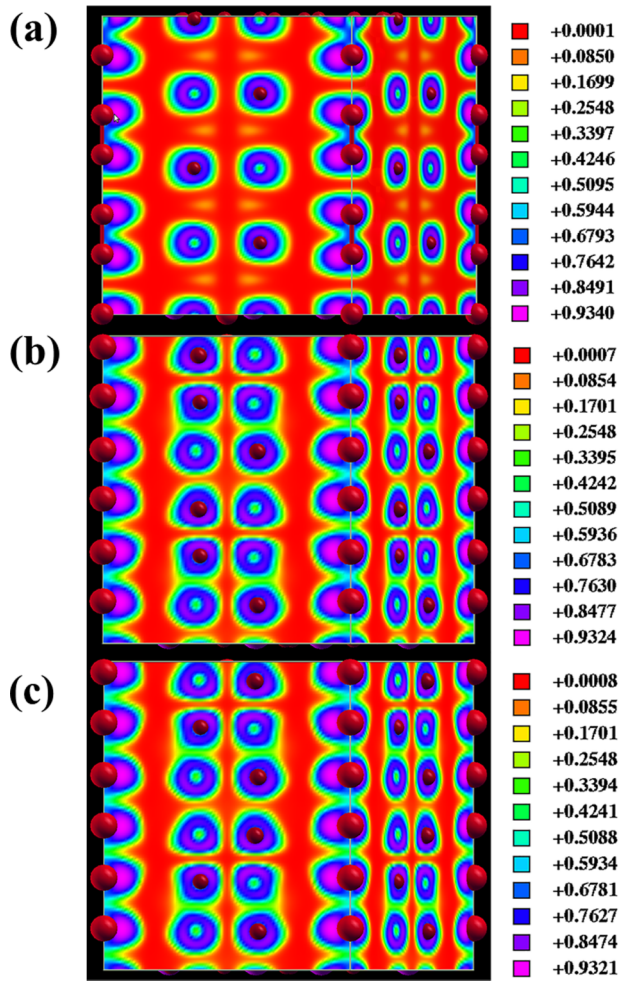

FIG. 8. Some representative images of the electron localization functions (ELFs) of Br@AFI at 0 (a), 19 (b), and 24 GPa (c), respectively. The atoms are as follows: big-sized and red balls for bromine atoms, small-sized and red balls for oxygen atoms, pink for aluminum atoms, and yellow for phosphorus atoms.

between the Br_2 molecules. At the same time, the charge between bonding bromine atoms is decreased compared with that observed in the low-pressure structure. This indicates that an increase in pressure averages the charge localization on the Br_2 molecules and promotes the formation of 1D bromine atomic chains at higher pressures. At pressures above 19 GPa, the intermolecular Br–Br distance decreases, and it becomes almost comparable to the intramolecular bond length in Br_2 molecules at 24 GPa (Figs. 7 and 8). This suggests that the 1D bromine atomic chains form at 24 GPa, and this result is further supported by the homogenization of the charge distribution in the linear structure, as shown in Fig. 8(c).

For bulk Br_2, it has been shown that the intramolecular distance first increases with increasing pressure up to about 25 GPa, and then decreases at higher pressures (Fig. 7), which suggests that a phase transition (phase I to phase I′) occurs.[8,23–25] This phase transition is suggested to be an intrinsic property of molecular bromine, and to result from subtle second-neighbor intermolecular interactions.[25] In contrast, compression causes the Br_2 molecules confined inside the 1D nanochannels in the present study to rotate

so that they lie along the 1D channel direction. This enhances the van der Waals interaction by reducing the distance between neighboring molecules. As a result, the intramolecular Br–Br distance (d_1 and d_3 in Fig. 7), which gradually increases with increasing pressure, becomes equal to the intermolecular distance between bromine species at 24 GPa. This suggests that the confined Br_2 molecules lose their molecular identity (molecular dissociation) and that the bromine atomic chains probably form at this pressure. At pressures above 24 GPa, the intramolecular distance gradually decreases. This variation in intramolecular distance for the confined Br_2 molecules is comparable to that observed for the bulk Br_2 molecules.[8,23–25] As illustrated above using theoretical simulations, nanoconfinement provides a strategy for the preparation of atomic chains under high pressure, although the evidence for the formation of a 1D bromine atomic chain is not clear from our Raman and XRD experimental studies. Further theoretical and experimental investigations are required to explore the physical dynamics of the atomic chains and the metallization of diatomic molecules under nanoconfinement at high pressures.

IV. CONCLUSIONS

In summary, we present the high-pressure behavior of bromine species confined in the nanochannels of AFI single crystals. Both experimental and theoretical studies suggest that high pressure can induce structural transformations in the confined bromine species, such as the growth of bromine chains at pressure above 3.7 GPa and molecular dissociation at about 24 GPa, and modify the inter- and intramolecular interactions. Furthermore, the pressure-prolonged bromine chains can be reversed inside the nanochannels of AFI single crystals at ambient pressure.

The present study also suggests that loading the diatomic Br_2 molecules into the nanospace of AFI single crystals can greatly enhance the structural stability of the host material, which has also been observed for I_2@AFI,[12] I_2@zeolite $AlPO_4$-11,[13] I_2@Si-46,[20] and N_2@AFI.[21] In some cases, however, the intercalated diatomic molecules do not affect the stability of the host structure [e.g., I_2@SWNT (single-wall carbon nanotubes)],[11] and may even reduce the structural stability of the host [e.g., Br_2@DWNT (double-wall carbon nanotubes)].[19] The difference may be related to the location of the diatomic molecules within the host materials,[11,19] their concentration,[19] or charge transfer between the molecules and the host material.[11,19] Further investigation of diatomic molecules intercalated in different compounds is required for a better understanding of this matter.

It is worth noting that nanoconfinement has an important effect on the high-pressure behavior of diatomic molecules, such as Br_2,[17–19] I_2,[11–13,16,20] and N_2.[21] Most importantly, the present study provides a strategy for tuning inter- and intramolecular interactions, and thus for the structural manipulation of diatomic molecules. This strategy may be able to shed new light on the mechanisms of diatomic molecular dissociation and metallization, as well as on the structural dynamics of 1D atomic and molecular wires in nanoconfinement.

SUPPLEMENTARY MATERIAL

See supplementary material for a second electron microprobe (SEM) image of the AFI single crystals; optical microscopic views of the Br@AFI single crystals; Raman spectra of Br@AFI synthesized with different reaction times and after the samples were kept in air for different amounts of time; polarized Raman spectra of Br@AFI; the fitting analysis of the Raman spectra of Br@AFI single crystals at various pressures; and the unit-cell parameters and volumes of doped AFI single crystals as a function of pressure.

ACKNOWLEDGMENTS

The authors thank P. Thiel for editing this manuscript, and two anonymous reviewers for their very constructive comments and helpful suggestions. This work was supported by the National Basic Research Program of China (Grant No. 2011CB808200), the NSFC (Grant Nos. 51025206, 51032001, 11504150, 11634004, and 51320105007), and the Cheung Kong Scholars Programme of China and Innovative Research Team in University (Grant No. IRT1132).

[1]K. Takemura, S. Minomura, O. Shimomura, and Y. Fujii, Phys. Rev. Lett. **45**, 1881 (1980).
[2]H. K. Mao and R. J. Hemley, Science **244**, 1462 (1989).
[3]K. A. Johnson and N. W. Ashcroft, Nature **403**, 632 (2000).
[4]M. Eremets, R. J. Hemley, H. K. Mao, and E. Gregoryanz, Nature **411**, 170 (2001).
[5]S. Desgreniers, Y. K. Vohra, and A. L. Ruoff, J. Phys. Chem. **94**, 1117 (1990).
[6]K. Takemura, K. Sato, H. Fujihisa, and M. Onoda, Nature **423**, 971 (2003).
[7]Y. Fujii, K. Hase, Y. Ohishi, H. Fujihisa, N. Hamaya, K. Takemura, O. Shimomura, T. Kikegawa, Y. Amemiya, and T. Matsushita, Phys. Rev. Lett. **63**, 536 (1989).
[8]T. Kume, T. Hiraoka, Y. Ohya, S. Sasaki, and H. Shimizu, Phys. Rev. Lett. **94**, 065506 (2005).
[9]D. Duan, Y. Liu, Y. Ma, Z. Liu, T. Cui, B. Liu, and G. Zou, Phys. Rev. B **76**, 104113 (2007).
[10]U. D. Venkateswaran, E. A. Brandsen, M. E. Katakowski, A. Harutyunyan, G. Chen, A. L. Loper, and P. C. Eklund, Phys. Rev. B **65**, 054102 (2005).
[11]L. Alvarez, J. L. Bantignies, R. Le Parc, R. Aznar, J. L. Sauvajol, A. Merlen, D. Machon, and A. San Miguel, Phys. Rev. B **82**, 205403 (2010).
[12]M. G. Yao, T. Y. Wang, Z. Yao, D. F. Duan, S. L. Chen, Z. D. Liu, R. Liu, S. C. Lu, Y. Yuan, B. Zou, T. Cui, and B. B. Liu, J. Phys. Chem. C **117**, 25052 (2013).
[13]S. L. Chen, M. G. Yao, Y. Yuan, F. X. Ma, Z. D. Liu, R. Liu, X. Yang, B. Liu, B. Zou, T. Cui, and B. B. Liu, Phys. Chem. Chem. Phys. **6**, 8301 (2014).
[14]V. V. Poborchii, A. V. Kolobov, J. Caro, V. V. Zhuravlev, and K. Tanaka, Phys. Rev. Lett. **82**, 1955 (1999).
[15]Z. K. Tang, D. Sun, J. Wang, J. Chen, and G. Li, Appl. Phys. Lett. **73**, 2287 (1998).
[16]J. T. Ye, Z. K. Tang, and G. G. Siu, Appl. Phys. Lett. **88**, 073114 (2006).
[17]P. C. Eklund, N. Kambe, G. Dresselhasu, and M. S. Dresselhasu, Phys. Rev. B **18**, 7069 (1978).
[18]B. B. Liu, Q. L. Cui, M. Yu, G. T. Zou, J. Carlsten, T. Wågberg, and B. Sundqvist, J. Phys.: Condens. Matter **14**, 11255 (2002).
[19]A. L. Aguiar, A. San-Miguel, E. B. Barros, M. Kalbáè, D. Machon, Y. A. Kim, H. Muramatsu, M. Endo, and A. G. Souza, Phys. Rev. B **86**, 195410 (2012).
[20]A. San-Miguel, P. Mélinon, D. Connétable, X. Blase, F. Tournus, E. Reny, S. Yamanaka, and J. P. Itié, Phys. Rev. B **65**, 054109 (2002).
[21]H. Lv, M. G. Yao, Q. G. Li, R. Liu, B. Liu, Z. Yao, D. D. Liu, Z. D. Liu, J. Liu, Z. J. Chen, B. Zou, T. Cui, and B. B. Liu, Sci. Rep. **5**, 13234 (2015).
[22]Z. D. Liu, M. G. Yao, Y. Yuan, S. L. Chen, R. Liu, S. C. Lu, B. Zou, T. Cui, and B. B. Liu, J. Raman Spectrosc. **46**, 413 (2015).
[23]A. San Miguel, H. Libotte, J. P. Gaspard, M. Gauthier, J. P. Itié, and A. Polian, Eur. Phys. J. B **17**, 227 (2000).

[24]A. San-Miguel, H. Libotte, M. Gauthier, G. Aquilanti, S. Pascarelli, and J.-P. Gaspard, Phys. Rev. Lett. **94**, 015501 (2007).
[25]M. Wu, S. T. John, and Y. Pan, Sci. Rep. **6**, 25649 (2016).
[26]H. Fujihisa, Y. Fujii, K. Takemura, and O. Shimomura, J. Phys. Chem. Solids **56**, 1439 (1995).
[27]A. P. Hammersley, S. O. Svensson, M. Hanfland, A. N. Fitch, and D. Hausermann, High Pressure Res. **14**, 235 (1996).
[28]S. B. Fagan, R. Mota, A. J. R. da Silva, and A. Fazzio, Phys. Rev. B **67**, 205414 (2003).
[29]S.-P. Huang, W.-D. Cheng, J.-M. Hu, Z. Xie, H. Hu *et al.*, J. Chem. Phys. **129**, 174108 (2008).
[30]H. D. Sun, Z. K. Tang, J. Chen, and G. Li, Appl. Phys. A **69**, 381 (1999).
[31]P. Baierl and W. Kiefer, J. Raman Spectrosc. **3**, 353 (1975).
[32]P.-G. Johannsen and W. B. Holzapfel, J. Phys. C: Solid State Phys. **16**, 1961 (1983).
[33]H. Lv, M. G. Yao, Q. G. Li, R. Liu, S. C. Lu, L. H. Jiang, W. Cui, Z. D. Liu, J. Liu, Z. J. Chen, B. Zou, T. Cui, and B. B. Liu, J. Appl. Phys. **111**, 112615 (2012).